



SIMPLIFIED VULNERABILITY ASSESSMENT OF HISTORICAL CITY CORES - THE EXAMPLE OF THE CITY OF XANTHI

D. Vamvatsikos¹ and S. J. Pantazopoulou²

ABSTRACT

A methodology is developed to address the problem of the collective seismic vulnerability of historical cities. Our focus is the derivation of fragility curves of simple structural models that represent an ensemble of historical masonry buildings. The structural model estimates lateral strength using a Mohr-Coulomb type failure criterion applied on the cross sectional area of load-bearing walls in the building's plan. Example data are drawn from the building population of the historical city of Xanthi, in Northeastern Greece. The seismic behavior of the simplified systems is efficiently assessed using approximate incremental dynamic analysis via static pushover. Monte Carlo simulation with latin hypercube sampling is applied to include the effect of epistemic uncertainties on the system performance. The result is a simple and efficient evaluation tool that can facilitate a comprehensive performance evaluation of groups of masonry structures in a seamless way that is consistent with current performance-based seismic assessment frameworks.

Introduction

The vulnerability of historical city cores is an important issue for numerous cities in seismic areas, a fact exemplified by the recent devastation of the city of L' Aquilla by the 2009 Abruzzo earthquake. Historical cores are typically composed of numerous buildings of stone masonry often built over different periods, with varying degrees of workmanship and usually in various degrees of disrepair. It is not surprising that quantifying their collective seismic vulnerability is not a simple problem. Actually, this has been a recurring issue of interest in the literature, where multiple research teams have made valuable contributions, especially in the context of modeling, some aiming towards more accurate and elaborate models and others towards simpler and more tractable ones.

For example, Tanrikulu et al (1992) have presented models of masonry structures under seismic excitation, while D' Ayala et al (1997) use simple mechanical models for a case-study of seismic loss estimation for the city of Lisbon. More recently, D' Ayala and Speranza (2003) have offered a comprehensive analysis of collapse mechanisms of masonry structures, geared towards

¹Lecturer, Dept. of Civil & Env. Engineering, University of Cyprus, P.O. Box 20537, Nicosia, 1678, Cyprus

²Professor, Dept. of Civil Engineering, Demokritos University of Thrace, Xanthi, 67100, Greece

capturing such effects with few equations. In essence, such attempts recognize the inherent uncertainty in the structures themselves and make do with lean, easily-calibrated models. Yet, what we believe is lacking in this context is the existence of an equally simple, yet accurate methodology to provide an educated estimate of the seismic vulnerability of such groups of structures while taking into account both record-to-record aleatory randomness and epistemic uncertainty due to the inherent lack of knowledge on the buildings. Working in accordance with recent advances in performance-based earthquake engineering frameworks (e.g. Cornell and Krawinkler 2000) we aim to provide such a methodology that remains easy to apply and we are going to use it on the unique case of the historical center of Xanthi.

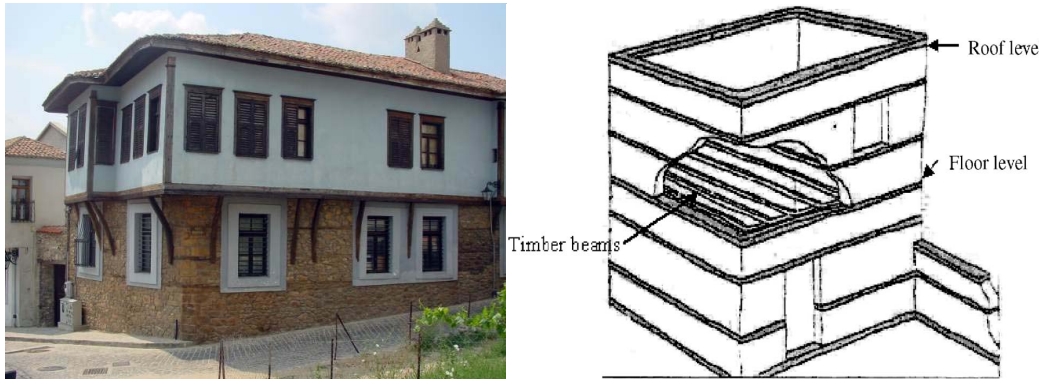


Figure 1. (a) Typical example of timber laced stone-masonry dwelling in Xanthi. (b) Layout of TLM (from Vintzileou 2008).

The old town of Xanthi

Xanthi is a historical urban center in Northeastern Greece in the province of Thrace, its origins being traced back to pre-Byzantine times (mentioned by Strabo, 1st century A.D.). Situated in an ecologically rich area protected by the Ramsar treaty, the city core represents today the most well preserved sample of traditional Balkan architecture surviving in Greece. The city was destroyed by successive earthquakes in the 1820-30s, and was vigorously rebuilt immediately after, becoming an important international tobacco production, processing and exporting center. The residential part of the city underwent a second phase of expansion after 1860 when the nearby administrative center of Genissea was devastated by widespread soil liquefaction after yet another strong earthquake. Structures built ranged from three storey clay-masonry storehouses and warehouses with stone masonry basements and large covered plan area (usually floor-diaphragms comprised steel I-beam traverses that encased clay masonry arches spanning between the parallel steel beams), to typical two storey residential dwellings built almost exclusively with the traditional load-carrying timber-laced masonry system abounding in the Balkans.

This structural system is actually known since the Roman times as *Opus Craticium*, but the origins of this construction archetype dates back to pre-Minoan times, and it continues through classical antiquity and the Roman times (Vitruvius 27-23 BC) up to the early 20th century in the Balkan region, when it was displaced by reinforced concrete (RC). In timber-laced masonry (TLM), lateral load resistance is imparted by interface friction between mortar and

stone or brick, and enhanced by the bearing action of gravity loads. Timber lacing (referred to hereon as *tiers*) acts in masonry walls as shear reinforcement, interrupting the planes of diagonal tension failure exactly in the same manner as horizontal reinforcing bars function as shear reinforcement in conventional RC walls (Tastani et al. 2009). Tiers are 0.1m thick timber beams embedded in the masonry parallel to the joints. A basic characteristic of this type of construction is the relatively large area ratio of exterior and interior walls, either reinforced or unreinforced with tiers, and the relatively flexible diaphragms. This characteristic imparts a great degree of robustness in the structure. Walls usually have an aspect ratio (height to length) of almost 1.0 (with the exception of piers forming between upper-storey windows) and therefore the behavior of the walls in their plane is dominated by shear deformation.

Today, an open issue in seismically active areas such as Northern Greece is assessment of seismic vulnerability of historical or traditional buildings. The traditional residential core of the city of Xanthi, which has been classified as protected heritage construction is such an example. Typical problems encountered in this process are (a) that the lateral load resisting system is undefined, (b) old construction often combines compounded effects due to ageing, so their actual material properties and condition cannot be estimated with certainty and (c) their great variability of form.

Mechanical model

TLM buildings of Xanthi, being entirely utilitarian, were built in the same chronological period with local methods and workmen and using locally produced materials from the quarry of the Kosynthos river. Thus, such residential houses present several typifying characteristics that fall within well defined ranges of values. The typical house is a two storey dwelling with storey height ranging from 2.6 to 3 m. The floor plan is nearly rectangular (sides ranging from 8 to 12 m), with floor area ranging between 60 and 130 m². The lower floor and the basement, if it exists, are constructed with perimeter stone masonry walls; wall thickness ranges from 550mm to 700mm. Thus, the typical floor plan contains an average 20% area of gravity load-bearing walls, with a considerably low standard deviation in the range of 10%.

Fig. 2 plots the average shear stress – strain diagram for stone masonry walls without tiers adopted by Eurocode 8-III. Shear strength, f_v , is estimated as a weighted product of compressive strength of building block strength f_{bc} and joint mortar compressive strength, f_{mc} : $f_v = 1.25k f_{bc}^{0.7} f_{mc}^{0.3}$ (stress terms in MPa, k in the range of 0.35 to 0.55). The range of values of the parameters listed above may vary, but the mean strength is estimated as 0.5MPa with a standard deviation of 0.15MPa. Note that the code recommended values for the shear distortion upon *yielding* of the masonry wall (yielding here is used to identify the onset of friction-sliding behavior along mortar joints after the occurrence of diagonal cracking) is in the range of 0.15%, whereas the shear strain ductility ranges reaching as high values as 3 in cases of timber laced masonry (EC8-III 2009).

The design code model for shear strength rides on a Mohr-Coulomb type of idealization of the behavior of stone masonry, according with which, the cracking shear strength, v_{Rd1} , of unreinforced masonry is expressed in terms of the inherent stone-binder cohesion, σ_z is the normal compressive stress clamping the potential sliding plane, and μ is the apparent frictional

coefficient.

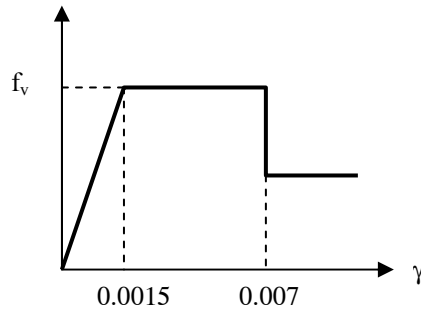


Figure 2. Code-recommended resistance curve for masonry walls.

$$v_{Rd1} = c + \mu \cdot \sigma_z \quad (1)$$

In obtaining the code relationship the frictional component of shear strength has been neglected on the assumption that normal stresses owing to overbearing loads are very small; this simplifies Eq. (1) to a Tresca-type failure criterion. The cohesion c may alternatively be taken as the weighted product of tensile (f_t') and compressive (f_c') strengths of the weaker component of the composite masonry (i.e., of the mortar): $c=0.5(f_t' f_c')^{0.5}$ (where f_t' is approximated as $0.1f_c'$); this approach yields commensurate results with those given earlier (conservatively around 0.5MPa). The contribution of tiers in this strength model is estimated by the total force, V_b , sustained by those tier elements that intersect a 45° plane of failure after diagonal cracking.

Equivalent Single Degree of Freedom Idealization

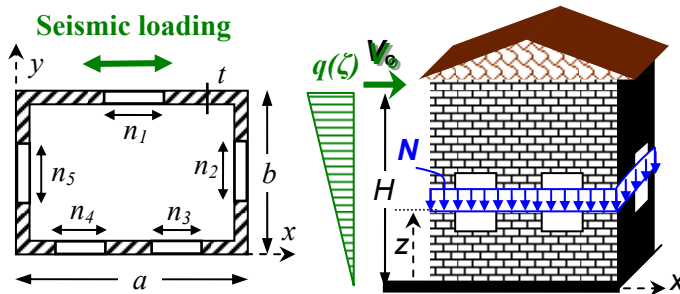


Figure 3. Seismic loading on a traditional masonry structure

Due to their low aspect ratio, robustness of load bearing structure and mode of construction (layered joints and building blocks), masonry walls develop insignificant flexural action in their plane of action, their fundamental mode of vibration approaching to a linear distribution of displacement with distance from the base; this corresponds to a shear-type behaviour, marked by an almost constant shear angle of distortion with height. This result is supported by 3-D finite element simulations of the outer shell of these structures; extreme diaphragm flexibility promotes the tendency of walls normal to the plane of action to also bend in the out of plane direction increasing the risk of a weak mode of failure with detachment of orthogonal walls at the corners. Considering the true complexity of the mechanical problem, the

uncertainty with regards the mechanical behavior of the materials, the extent of damage, and the actual state of interaction that occurs at the interfaces of different materials (e.g., timber and mortar or stones, soil with masonry, etc.) any calculation-intensive approach would be incompatible with the actual level of confidence in the input values. For this reason, response is considered in the fundamental mode of vibration only, as it may be easily shown that for a cantilever structure where the shear deformation is higher than the flexural contribution, the mass participating in this fundamental mode is at least 80% of the available mass, whereas the fundamental mode is almost linear height-wise. Seismic forces are distributed over the height of the structure as illustrated in Fig. 3. There is a linear distribution, $q(z)$, following the fundamental shape of vibration, and a concentrated force at the top of the structure V_o associated with the roof weight. Equivalent mass (for overturning moments) and stiffness of the system are given as,

$$M = \int_0^H m(z) \left(\frac{z}{H} \right)^2 dz + M_{roof}; \quad K = \int_0^H k_w A_w \left(\frac{1}{H} \right)^2 dz \quad (2)$$

where, k_w represents the secant wall stiffness in the shear-stress – distortion diagram, Fig. 3, A_w the area of the load bearing walls in the floor plan, and H the total height of the structure. The mass $m(z)$ per unit height of the structure is evaluated from the wall thickness and the specific gravity of the stone blocks, γ_w (ranging between $\gamma_w = 20$ to 27 kN/m^3). There is also the weight of the roof taken as $\gamma_r A_r$; A_r is the roof area, and γ_r is the unit area weight of the roof, ranging from $\gamma_r = 160-180 \text{ Kg/m}^2$ for stone tiles, to $\gamma_r = 110 - 150 \text{ Kg/m}^2$ for roman-type and byzantine-type ceramic tiles. These values include the self weight of timber trusses, sheathing and insulation. The tributary roof weight is transferred to the supporting walls according to the geometry of the roof (two-way or four-way). Note that the wall cross sectional area, A_w may be altered with z due to the presence of openings. Here, for simplicity and with no loss of generality, A_w is assumed constant with regards to the definition of the axial load.

Building Ensemble Probabilistic Characterization

All in all, the proposed model consists of 11 random parameters which have been introduced above and from which all other essential variables may be derived. These appear in Table 1. The 11 parameters are considered statistically independent with the only exception of θ_y and μ_u , i.e., the yield shear strain and the ultimate ductility, respectively, which have a positive correlation of 0.75. This reflects the fact that stiffer walls tend to have lower ductilities compared to softer ones. These two values, together with the shear strength f_v , offer a complete characterization of the stress-strain curve of masonry (Fig.2) up to the significant drop in strength that signals major damage in the wall. Thereafter, the uncertainty in the response and the scarcity in the data is such that we choose to ignore the contribution of this residual segment to the strength of the wall.

The distributions of the above variables have been estimated using experimental results in the literature, expert opinion and data from an inventory of Xanthi buildings. For lack of a better model, we have assumed almost all parameters to be normally distributed with truncation limits at some reasonable minimum and maximum limit, selected according to available data in order to avoid any problems with the normal distribution providing very small or very large unrealistic values.

Having these values at our disposal, we can easily derive the essential variables needed for our problem. First is the roof weight per unit area, γ_r which is equal to γ_{rc} if $r_{type} \leq 0.5$ or equal to γ_{rs} if $r_{type} > 0.5$. In other words, this follows a bimodal distribution which is a 50-50 mixture of two (truncated) normals. Then, the total building weight W that is effective for shear loading is estimated as the sum of the weight of the walls, the roof, the factored live load $q=2\text{kN/m}^2$ and a 0.2kN/m^2 dead-load surcharge for floors and other structural elements left out. The other needed quantities are the yield base shear V_y , the ultimate shear strain θ_u , the first-mode spectral acceleration at yield $S_{ay}(T_1, \xi)$, the elastic stiffness K_{el} and the first mode period T_1 :

$$\begin{aligned}
 W &= A(\gamma_w p_w H + \gamma_r + 0.3q + 0.2) \\
 V_y &= 0.5 f_v p_w A \\
 S_{ay}(T_1, \xi) &= \frac{V_y}{W} \\
 \theta_u &= \mu_u \theta_y \\
 K_{el} &= \frac{V_y}{\theta_y H} \\
 T_1 &= 2\pi \sqrt{\frac{W}{gK_{el}}}
 \end{aligned} \tag{3}$$

Table 1. The characterization of the parameters of the probabilistic model for an ensemble of TLM buildings from Xanthi.

Parameter	Symbol	Mean	c.o.v.	min	max	Distribution
wall shear strength	f_v (MPa)	0.50	30%	0.20	0.80	Tr. Normal
plan area	A (m ²)	90	22%	60	130	Tr. Normal
ratio of walls in plan	p_w	0.20	10%	0.16	0.24	Tr. Normal
total height	H (m)	5.6	5%	5.2	6.0	Tr. Normal
yield shear strain	θ_y	0.0015	25%	0.0010	0.0030	Tr. Normal
ultimate ductility	μ_u	2.0	25%	1.2	3.2	Tr.. Normal
damping ratio	ξ	0.05	30%	0.03	0.07	Tr. Normal
specific gravity of stones	γ_w (kN/m ³)	24	10%	20	27	Tr. Normal
stone tiles' roof weight	γ_{rs} (kN/m ²)	1.7	5%	1.6	1.8	Tr. Normal
ceramic tiles' roof weight	γ_{rc} (kN/m ²)	1.3	10%	1.1	1.5	Tr. Normal
type of roof	r_{type}	0.5	-	0	1	Uniform

Performance Evaluation via IDA and SPO2IDA

To evaluate the seismic performance of the equivalent single-degree-of-freedom (SDOF) systems we employ Incremental Dynamic Analysis (IDA, Vamvatsikos and Cornell 2002). This would normally involve performing a series of nonlinear dynamic analyses under a multiply scaled suite of ground motion records. By selecting proper Engineering Demand Parameters (EDPs) to characterize the structural response and choosing an Intensity Measure (IM), e.g. the 5% damped first-mode spectral acceleration $S_a(T_1, 5\%)$, to represent the seismic intensity, we

can generate the IDA curves of EDP versus IM for each record and the 16%, 50% and 84% summarized curves, representing the aleatory randomness attributed to the record-to-record variability. On such curves the desired limit-states can be defined by setting appropriate limits on the EDPs allowing the estimation of the corresponding capacities and their probabilistic distribution. Such results can be combined with probabilistic seismic hazard analysis to evaluate the mean annual frequencies (MAFs) of exceeding the limit-states thus offering a direct characterization of seismic performance.

Nevertheless, IDA comes at a considerable cost, even for simple structures, necessitating the use of multiple nonlinear dynamic analyses that are usually beyond the abilities and the computational resources of the average practicing engineer. A fast and accurate approximation has been recently proposed for IDA, both for single and multi-degree-of-freedom systems utilizing information from the force-deformation envelope (or backbone) to generate the summarized 16%, 50% and 84% IDA curves by using elaborate fitted equations (Vamvatsikos and Cornell 2006). The approximation is based on the study of numerous SDOF systems having varied periods, moderately pinching hysteresis and 5% viscous damping, while they feature backbones ranging from simple bilinear to complex quadrilinear with an elastic, a hardening and a negative-stiffness segment plus a final residual plateau that terminated with a drop to zero strength as shown in Figure 1 (Ibarra et al. 2005). The oscillators were analyzed through IDA and the resulting curves (Fig. 2) were summarized into their 16, 50, and 84% fractile IDA curves which were in turn fitted by flexible parametric equations. Having compiled the results into the SPO2IDA tool, available online (Vamvatsikos 2002), we can get an accurate estimate of the performance of virtually any oscillator without having to perform the costly analyses, almost instantaneously recreating the fractile IDAs in normalized coordinates of $R = S_a(T, 5\%) / S_{ay}(T, 5\%)$ (where $S_{ay}(T, 5\%)$ is the $S_a(T, 5\%)$ value to cause first yield) versus ductility μ .

Having SPO2IDA available we can easily perform a Monte Carlo simulation by randomly varying the parameters of the oscillator according to their distribution (Vamvatsikos 2007). Due to the simple backbone of our equivalent SDOF system, the uncertain parameters considered in normalized coordinates are only the ultimate ductility μ_u and the period T of the oscillator. By using a latin hypercube sampling scheme (McKay 1979) to draw from their distributions and applying SPO2IDA on each alternate model we are able to efficiently incorporate the epistemic uncertainty into the IDA results without actually performing a single dynamic analysis. The final results are the distributions of the estimates of fractile demands and capacities, allowing the assessment of confidence intervals or dispersion β -values for the oscillator R -capacities given μ or the μ -demands given the normalized intensity R .

Such values can be de-normalized to more meaningful quantities of roof displacement and S_a to present us with the typical IDA curves (Vamvatsikos and Cornell 2005). Particular care needs to be exercised when trying to combine values coming from sample buildings with different first-mode period and damping. In order to provide a single base of reference we will translate all such results to a common IM, being the $S_a(T_{1b}, 5\%)$ where $T_{1b}=0.17s$ is the first-mode period of the base case building, i.e., the building defined by the central values of all random parameters.

Analysis Results and Discussion

The results from applying SPO2IDA on $N_{MC}=200$ samples of buildings from the Xanthi probabilistic model appear in Fig.4. The corresponding 200 static pushover curves are in Fig.4a showing the impact of the positive correlation between θ_y and θ_u : They are either stiff and with high yield strength or show lower strengths but higher ductilities. The corresponding 200 median IDAs from SPO2IDA appear in Fig.4b and show the actual distribution of response expected from the structure. Their spread characterizes almost entirely the effect of epistemic uncertainty on the central demand and capacity of the structures.

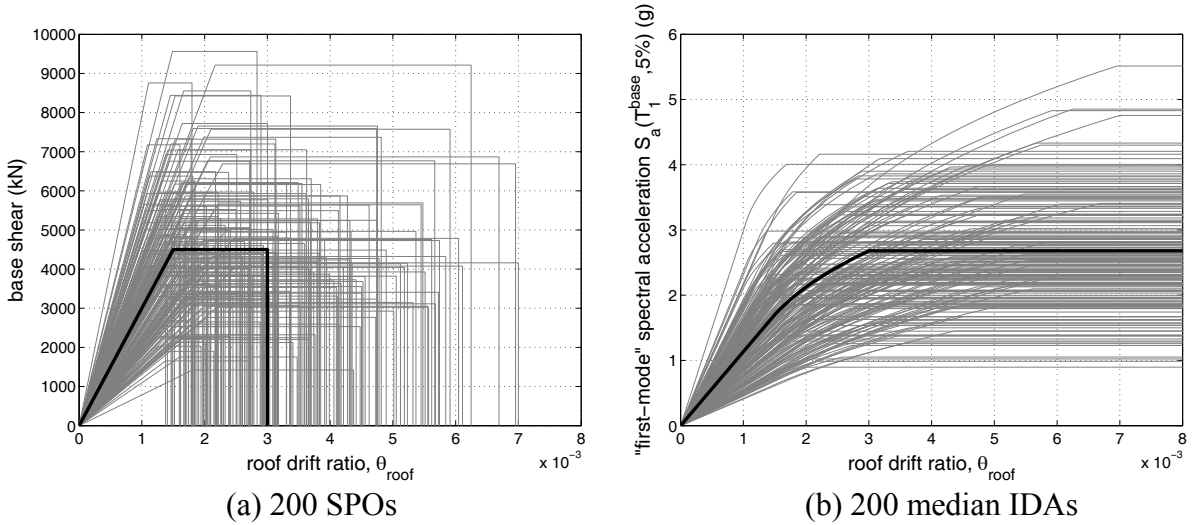


Figure 4. (a) The resulting pushovers from of simulation and (b) the corresponding median IDAs produced through SPO2IDA.

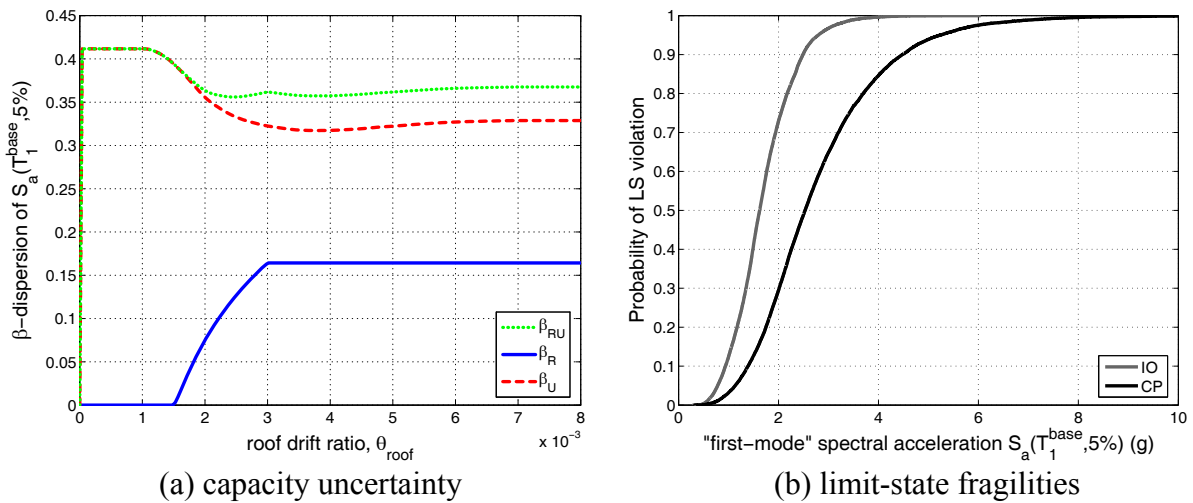


Figure 5. (a) The aleatory randomness and epistemic uncertainty in Sa-capacity for given values of θ_{roof} and (b) the corresponding fragility curves produced for two limit-states.

To better illustrate the results of our case-study, we show the derived values of record-to-record variability β_R , estimated as one half the difference between the 16%, 84% S_a -capacities of the base case for given value of roof drift, versus the epistemic uncertainty β_U derived as the log-standard deviation of the median IDAs in Fig.4b. The two are combined into the total variability β_{RU} that is of major importance for accurate performance evaluation. This can be done either via a square-root-sum-of-squares (SRSS) rule or directly by simulating individual records, say 50, from the S_a -capacity distribution of each sample structure and taking the overall log-standard deviation of the 50x200=10000 resulting individual IDA curves. Due to the correlation present in the results, the latter is actually the better method, as the SRSS rule may lead up to a 25% error.

Finally, we have produced the fragility curves in Fig 5b for two limit-states, one signifying the onset of damage at first-yield, termed Immediate Occupancy (IO), and another at the loss of strength that signifies near-collapse, termed Collapse Prevention (CP). It is important to note that the definition of the limit-states is not based on a unique, externally-supplied response value of the roof drift θ_{roof} but instead it is completely model-dependent. In other words, when each model exceeds its own θ_y value, it exceeds the IO state, and when it exceeds its θ_u it also violates CP. This is in direct contrast with many recent applications of performance-based earthquake engineering based on the PEER framework (Cornell and Krawinkler 2000), where it is usually assumed that the distribution of damage for any structural component is not correlated in any way to the actual capacity such a component might have in the structural model used to derive its response by static or dynamic analysis.

While the fragility curves in Fig 5b are most useful in combination with a complete seismic hazard curve, we can derive some useful results considering the typical earthquake intensity defined in the current seismic code of Greece for the city of Xanthi (GSC 2000). These amount to about 0.45g for $T_{1b}=0.17$ sec and a 10% in 50yrs event. This corresponds to a negligible probability of exceeding CP and a low probability of violating IO. Thus, some serviceability-level damages are possible, but the building stock seems to be safe from any major collapses. Of course, such conclusions should be taken with a grain of salt, considering the limits of our modeling and in light of any improvements that need to be done to calibrate it with recent experimental data.

Conclusions

A simplified methodology has been presented for the seismic vulnerability evaluation of a group historical structures. Using a simple mechanical model with appropriate probabilistic characterization based on existing literature, inventory data and expert opinion, we were able to derive fragility curves for the relatively homogeneous ensemble of stone masonry structures that comprise the historical core of the city of Xanthi. The end result is a realistic representation of the vulnerability of the building ensemble that incorporates both aleatory randomness and epistemic uncertainty in a concise and accurate way, showing that at the city center is vulnerable to serviceability-level damages from the design-level earthquakes occurring in the region, but, generally speaking, safe from catastrophic collapse.

References

- CEN, 2004. Eurocode 8: Design of structures for earthquake resistance Part 3: Assessment and retrofitting of buildings. June 2004, Doc. CEN/TC250/SC8/N388B. Comité Européen de Normalisation, Bruxelles.
- Cornell C. A., and H. Krawinkler, 2000. Progress and challenges in seismic performance assessment, *PEER Center News* 3 (2) URL <http://peer.berkeley.edu/news/2000spring/index.html>, [Oct 2009].
- D'Ayala D., and E. Speranza, 2003. Definition of Collapse Mechanisms and Seismic Vulnerability of Historic Masonry Buildings, *Earthquake Spectra* 19 (3) 479–509.
- D'Ayala D., R. Spence, C. Oliveira, and A. Pomonis, 1997. Earthquake Loss Estimation for Europe's Historic Town Centres. *Earthquake Spectra*, 14 (4) 773–793.
- Dolsek M. Incremental dynamic analysis with consideration of modelling uncertainties *Earthquake Engineering and Structural Dynamics* 2009; 38(6):805–825.
- Fragiadakis M., and D. Vamvatsikos, 2010. Fast Performance Uncertainty Estimation via Pushover and Approximate IDA, *Earthquake Engineering and Structural Dynamics* (in press).
- GSC, 2000. *Greek Seismic Code*, Ministry of Environment, Land and Public Works, Athens, Greece.
- Ibarra, L.F., R.A. Medina, and H. Krawinkler, 2005. Hysteretic models that incorporate strength and stiffness deterioration, *Earthquake Engineering and Structural Dynamics* 34 (12) 1489–1511.
- Liel A. B., C. B. Haselton, G. G. Deierlein, and J. W. Baker, 2009. Incorporating modeling uncertainties in the assessment of seismic collapse risk of buildings, *Structural Safety* 31 (2) 197–211.
- McKay M. D., W. J. Conover, and R. Beckman, 1979. A comparison of three methods for selecting values of input variables in the analysis of output from a computer code. *Technometrics* 21(2) 239–245.
- Tanrikulu A.K., Y. Mengi, and H.D. McNiven, 1992. The nonlinear response of unreinforced masonry buildings to earthquake excitation, *Earthquake Engineering and Structural Dynamics* 21 965–985.
- Tastani S., M. Papadopoulos, and S. Pantazopoulou, 2009. Seismic response of traditional masonry buildings: parametric study and evaluation, *Proceedings of the 1st International Conference on Protection of Historical Buildings*, Rome, Italy.
- Vamvatsikos D., 2002. SPO2IDA software for all periods. http://blume.stanford.edu/pdf/Tech%20Reports/TR151_spo2ida-allt.xls [May. 20, 2009].
- Vamvatsikos D., and C. A. Cornell, 2002. Incremental Dynamic Analysis, *Earthquake Engineering and Structural Dynamics* 31 (3) 491–514.
- Vamvatsikos D., and C.A. Cornell, 2005. Direct estimation of the seismic demand and capacity of MDOF systems through Incremental Dynamic Analysis of an SDOF Approximation, *ASCE Journal of Structural Engineering* 131 (4) 589–599.
- Vamvatsikos D., and C.A. Cornell, 2006. Direct estimation of the seismic demand and capacity of oscillators with multi-linear static pushovers through Incremental Dynamic Analysis. *Earthquake Engineering and Structural Dynamics* 35 (9) 1097–1117.
- Vamvatsikos D., 2007. Influence of parameter uncertainties on the seismic performance of oscillators via SPO2IDA, *Proceedings of the 10th International Conference on Applications of Statistics and Probability in Civil Engineering*, Tokyo.
- Vamvatsikos D., and M. Fragiadakis, 2010. Incremental dynamic analysis for estimating seismic performance uncertainty and sensitivity, *Earthquake Engineering and Structural Dynamics* (in press).
- Vintzileou E., 2008. The effect of timber ties on the behaviour of historic masonry, *ASCE Journal of Structural Engineering* 134 (6) 961–972.